Enhancement of Intracavity-Pumped Terahertz Parametric Oscillator Power by Adopting Diode-Side Pumped Configuration Based on KTiOPO$_4$ Crystal

Feilong Gao , **Xingyu Zhang** *, **Zhenhua Cong, Zhaojun Liu, Xiaohan Chen, Zengguang Qin, Peng Wang, Jinjin Xu, Zecheng Wang and Na Ming**

School of Information Science and Engineering, Shandong Provincial Key Laboratory of Laser Technology and Application, Shandong University, Qingdao 266237, China; 201520237@mail.sdu.edu.cn (F.G.); congzhenhua@sdu.edu.cn (Z.C.); zhaojunliu@sdu.edu.cn (Z.L.); cxh@sdu.edu.cn (X.C.); qinzengguang@sdu.edu.cn (Z.Q.); 201712312@mail.sdu.edu.cn (P.W.); 201732375@mail.sdu.edu.cn (J.X.); 201920408@mail.sdu.edu.cn (Z.W.); 201920404@mail.sdu.edu.cn (N.M.)
* Correspondence: xyz@sdu.edu.cn

check for updates

Abstract: In this paper, a KTiOPO$_4$ (KTP) crystal is used as the nonlinear medium in an intracavity-pumped terahertz parametric oscillator (TPO) based on stimulated polariton scattering (SPS). Almost all the reported intracavity SPS sources adopt the diode-end pumped configuration, and the THz output power is limited by the serious thermal effect and small fundamental beam size. For improving the THz output power, we propose diode-side pumping for the laser medium to get a higher fundamental power and a larger fundamental beam size. A convex–plane fundamental laser resonator is used to further offset the thermal effect and increase the fundamental beam size. The THz frequency of the intracavity-pumped KTP terahertz parametric oscillator can be discontinuously tuned from 3.19 THz to 5.94 THz with three gaps. The fundamental beam diameter in the KTP crystal is about 1.3 mm. The maximum average THz power is 166 µW at 5.74 THz under a pulse repetition frequency (PRF) of 6 kHz and a diode pump power of 98 W. By means of the diode-side pumped configuration, the maximum THz output power is more than two-fold higher compared to the diode-end pumped configuration reported using the KTP crystal.

Keywords: KTiOPO$_4$ crystal; terahertz parametric oscillator; nonlinear optics; diode-side pumping

1. Introduction

KiTiOPO$_4$ (KTP) is an outstanding optical nonlinear medium. It has many excellent properties such as a large nonlinear coefficient (d_{33} = 15.4 pm/V) [1], high optical damage threshold (10 J/cm^2 at 10 Hz, 6 ns, 1064 nm) [2], high transparency range, etc. The KTP crystal is used as a nonlinear medium to extend the wavelength range of a practical laser source. It has good performance in second-order nonlinear effects such as second harmonic generation (SHG) [3,4], sum frequency generation (SFG) [5,6], and optical parametric oscillation (OPO) [7,8], and third-order nonlinear effects such as stimulated Raman scattering (SRS) [9,10].

In recent years, researchers found that the KTP crystal could also be used to obtain THz radiation through the stimulated polariton scattering (SPS) effect [11–14]. SPS is a special frequency down-converting process which includes both second-order and third-order nonlinear effects [15]. When a strong pump wave (usually in the near-infrared range) is incident into the polar crystal which is both infrared-active and Raman-active, a near-infrared wave called a Stokes wave and a far-infrared wave with THz frequency are parametrically generated according to the energy conservation law and

the momentum conservation law. Because the refractive index of the nonlinear crystal in the THz wave spectral range is large, the SPS process must obey the non-collinear phase matching condition.

In 2014, Wang reported an external cavity-pumped SPS source using a KTP crystal. This is the first time that a nonlinear medium different from the traditional crystal LiNbO$_3$ (LN) was realized to generate THz radiation based on SPS. Different from the THz frequency of 0.6–3.5 THz obtained from the LN crystal [16–20], the generated THz frequency could be tuned from 3.17 THz to 6.13 THz by using the KTP crystal. The obtained THz pulse energy was 336 nJ at 5.72 THz when the pulse repetition frequency (PRF) was 10 Hz and the pump pulse energy was 80 mJ [11]. In the following years, there were some reports of enhancing the performance of the external cavity-pumped SPS laser using a KTP crystal [12–14]. The external cavity-pumped SPS sources are mainly used to generate terahertz pulses with relatively high pulse energy and low pulse repetition rate.

Compared with the external cavity-pumped system which requires a high-pulse-energy pumping laser, an intracavity-pumped system, in which the nonlinear crystal is inserted in the fundamental cavity, can take advantage of the high intracavity fundamental power density to enhance nonlinear conversion. Intracavity-pumped SPS sources are usually compact and exhibit relatively low SPS thresholds, high pulse repetition rates, high average THz output powers, and high diode-to-THz conversion efficiencies. The KTP crystal is also used as the nonlinear medium in intracavity-pumped SPS sources. Ortega reported an intracavity-pumped SPS laser using a KTP crystal in his PhD thesis. The diode-end pumped configuration for fundamental gain medium was adopted. The generated average THz power was 70.9 µW at 5.58 THz for a diode power of 7.3 W [21].

This diode-end pumped configuration is used in nearly all intracavity SPS sources [22–27]. Although the laser threshold is low and the diode-to-THz conversion efficiency is high in the diode-end pumped configuration because of the high overlapping efficiency between the diode wave and the fundamental wave, further improving the THz output power is difficult for several reasons. Firstly, the generations of the Stokes and THz waves arise from the consumption of the fundamental wave. In the diode-end pumped configuration, the diode power and the intracavity fundamental power are limited by the thermal fracture of the laser material [28]. Secondly, the SPS process must obey the non-collinear phase matching condition. The interaction volume among the fundamental, Stokes, and THz beams is positively correlated with the fundamental beam size and the overlap of the non-collinear Stokes beam (see Figure 1). However, the fundamental diameter in the diode-end pumped configuration is usually as small as several hundred micrometers. Diode-side pumping for the laser medium is an outstanding method to obtain high output power. It is used in the fields of single-mode laser [29,30], second harmonic generation [31,32], and stimulated Raman scattering [33,34]. Because the diode laser is uniformly incident into the laser rod, the thermal effect is relatively light in the diode-side pumped configuration. Thus, the system can operate efficiently even under high diode power [35]. In addition, the fundamental beam size is larger compared with that in the diode-end pumped configuration [36]. Of course, it should be pointed out that the diode-side pumped systems have the common disadvantage that the optical-to-optical efficiency is lower due to the insufficient absorption of the diode pump light in the outer part of the laser rod.
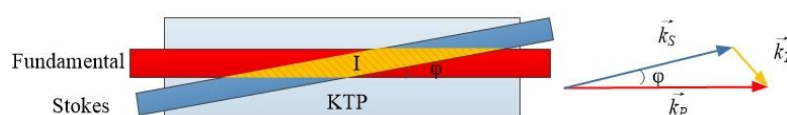
Figure 1. The spatial interaction between the fundamental and Stokes waves, and the non-collinear phase-matching condition.

In this paper, a KTP crystal was used as the nonlinear medium in an intracavity SPS source. The fundamental beam size and fundamental power were increased by means of side pumping for the laser medium to enhance the THz output power. The fundamental cavity was designed as a plane–convex configuration to further increase the fundamental beam size and offset some of the thermal

effect. Finally, the fundamental beam diameter in the KTP crystal was about 1.3 mm. The terahertz wave frequency could be intermittently tuned from 3.19 to 5.94 THz with three gaps. The obtained maximum THz average power was 166 µW at 5.74 THz under a diode power of 98 W and a PRF of 6 kHz. The maximum THz output power was more than two-fold higher compared to that obtained in the intracavity-pumped SPS laser using a KTP crystal with diode-end pumped configuration.

2. Experimental Set-Up

Figure 2 depicts the experimental schematic of the intracavity-pumped KTP terahertz parametric oscillator (TPO). Diode-side pumping for the gain medium of neodymium-doped yttrium aluminum garnet (Nd:YAG) was adopted. The diameter and length of the Nd:YAG rod (doping concentration of 1 at.%; anti-reflection coated at 1064 nm) were 3 mm and 65 mm, respectively. The maximum power of the diode laser was 180 W. The fundamental laser was Q-switched by an acousto-optic module (Gooch and Housego Company, Ilminster, Somerset, United Kingdom) which was coated with an anti-reflection (AR) film at 1064 nm. The fundamental resonator was composed of M1, M2, and the total reflection surface of the KTP crystal. Compared with the reported intracavity-pumped terahertz parametric sources in which the fundamental resonators were plane–plane or plane–concave configurations, the fundamental cavity was a convex–plane configuration. This could offset the thermal effect to some degree and further increase the fundamental beam size. The total fundamental cavity length was 320 mm. Mirror M1 was convex with a curvature radius of 2000 mm. It was coated with a high-reflection (HR) film at 1064 nm ($R > 99.9\%$). The output mirror M2 was flat with a reflectivity of 99.54% at 1064 nm. The Stokes cavity consisted of two plane mirrors (M3 and M4), and the cavity length was 100 mm. In order to avoid clipping the fundamental beam, M3 and M4 were processed as the same semicircle shape. M3 was HR coated from 1060 nm to 1100 nm ($R > 99.9\%$), and M4 was partial transmission coated from 1060 nm to 1100 nm ($T = 20\%$ at 1086 nm). The KTP crystal had an isosceles trapezoid shape in the xy plane, and the base angle was designed to be about 60°. The two waist planes of the KTP crystal were the optical windows for the fundamental and Stokes waves, and they were AR coated from 1060 nm to 1100 nm. This special shape allowed the THz wave to be radiated nearly perpendicularly through the base plane of the KTP crystal with no need for any couplers, and it allowed the fundamental and Stokes waves to be totally reflected on the THz output surface. The waist and base lines of the isosceles trapezoid were 15 mm and 26 mm, respectively. The thickness of the KTP crystal was 7 mm. The Stokes cavity mirrors were installed on two independent electromechanical rotating platforms. The tuning characteristics of the Stokes and THz waves could be realized by precisely controlling the axis of the Stokes cavity. The THz signal was received by a calibrated Golay cell (Tydex, GC-1D, Saint Petersburg, Leningrad Region, Russia). In order to avoid the interference of the undesired signals, a long-pass filter (TYDEX, LPF14.3-47, Saint Petersburg, Leningrad Region, Russia) was installed in front of the Golay cell. The duty cycle and operation frequency of the chopper between the THz output surface and the Golay cell were 50% and 10 Hz, respectively.
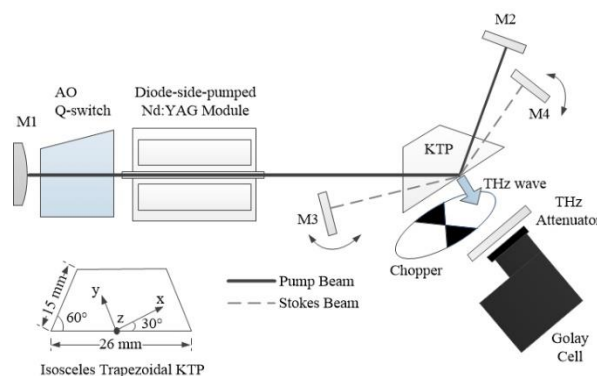
Figure 2. Experimental set-up of the intracavity-pumped terahertz parametric oscillator (TPO) using a KTiOPO$_4$ (KTP) crystal with diode-side pumped configuration.

3. Results and Discussion

The tuning characteristics of the intracavity KTP TPO with diode-side pumped configuration were investigated under a diode power of 80 W and a PRF of 6 kHz, as shown in Figure 3. A spectrometer (YOKOGAWA, AQ6315, 350–1750 nm, Musashino-shi, Tokyo, Japan) was used to monitor the Stokes wavelength. The generated Stokes wavelength was discretely tuned from 1076.3 to 1077.4 nm, from 1080.3 to 1081.6 nm, from 1082.6 to 1083.2 nm, and from 1085.4 to 1087.1 nm. The THz frequency was calculated using the energy conservation law and was tuned from 3.19 to 3.45 THz, from 4.21 to 4.53 THz, from 4.80 to 4.94 THz, and from 5.51 to 5.94 THz, respectively. There existed three gaps corresponding to the three A_1 transverse modes of the KTP crystal at 134, 154, and 179 cm^{-1}. The absorption for the electromagnetic wave is very large when the frequency is close to those variation modes. The optimal THz frequency was at 5.74 THz where the THz output power was maximal.
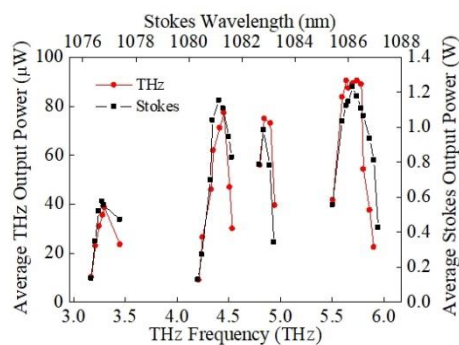
Figure 3. Tuning characteristics of the intracavity diode-side pumped KTP stimulated polariton scattering (SPS) laser.

The shaded area I in Figure 1 depicts the interaction area between the fundamental and Stokes beams in the crystal. The diagram is sketched for linear geometry for simplicity. The interaction area is the same as for a surface-emitted configuration because of the mirror reflection. The fundamental wave was perpendicularly incident into the crystal. The Stokes wave oscillated at an angle φ with the fundamental beam according to the near-forward scattering configuration $X(ZZ)X + \varphi$ in the SPS process [37]. The THz wave was generated in the overlapping area I. Obviously, as the fundamental beam size increases in size, so does the overlapping volume among the fundamental, Stokes, and THz waves in the crystal. In particular, for the KTP crystal, the optimal phase-matching angle between the fundamental and Stokes beams (2.4° in the crystal) is larger than that in LN and RbTiOPO$_4$. Thus, the fundamental beam size is more critical to the performance of the KTP SPS laser. The fundamental beam size outside the resonator was measured using a camera beam profiler (THORLABS, BC106N-VIS/M, 350–1100 nm, Newton, New Jersey, United States). The beam radii at different positions were fitted into the curve $\omega^2(x) = \omega_0^2[1 + (x/f)^2]$, where x represents the distance between the camera beam profiler and the output coupler M2, ω_0 is the beam waist radius, $f = \pi\omega_0^2/(\lambda M^2)$ is called the Rayleigh length, M^2 is the beam quality parameter, and λ is the wavelength. After curve fitting, we could obtain ω_0. Through the ABCD transformation, the fundamental beam diameter inside the KTP crystal could be calculated. The fundamental beam size decreased slightly with increasing diode power. When the diode power was increased from 60 W to 95 W, the fundamental beam size varied from 1.34 mm to 1.25 mm. The average M^2 values of the fundamental wave in the horizontal and vertical directions were measured at about 2.31 and 2.85, respectively, using an M^2 beam quality analysis system (THORLABS, M2MS, 400–5000 nm, Newton, New Jersey, United States).

The average output powers of the fundamental (before and after depletion), Stokes, and THz waves versus the diode power are shown in Figure 4 when the THz wave was at the optimal frequency of 5.74 THz, and the PRF was 6 kHz. By adjusting mirror M4, the SPS process could be switched on

and off to control the consumption of the fundamental wave and the generation of the Stokes and THz waves. When the diode pump power was 64 W, the fundamental wave began to be consumed, and the Stokes and THz waves were generated simultaneously. With increasing diode power, the residual fundamental power was nearly invariant at a level of about 600 mW, but the fundamental consumption rate (the fundamental consumption power divided by the original fundamental power) increased. When the diode pump power increased to 98 W, the fundamental output powers before and after depletion were measured at 1.33 W and 650 mW respectively, and the corresponding fundamental wave consumption increased to 51%. For improving the intracavity fundamental power, the transmission of the fundamental output mirror M2 at 1064 nm was designed to be very low (T = 0.46%). The one-way fundamental powers in the cavity before and after consumption were calculated as 289 W and 141 W, respectively. The average THz and Stokes output powers increased nearly linearly with increasing diode power. The average THz output power increased to 166 μW for a diode power of 98 W. A higher diode power was not tried in consideration of the optical damage threshold of the KTP crystal. The diode-to-THz conversion efficiency in this paper is relatively low compared with that in the reported diode-end pumped configuration based on the KTP crystal. However, the maximum average THz output power was more than doubled (166 μW versus 70.9 μW).
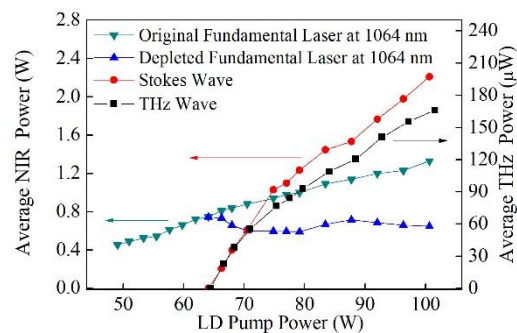
Figure 4. Input–output characteristics of the intracavity KTP SPS laser with diode-side pumped configuration.

The beam patterns of the original fundamental, depleted fundamental, and Stokes waves are shown in Figure 5 when the diode power was 98 W. Because of the diode-side pumped configuration, the beam quality of the fundamental wave was not very good. The mode structure of the fundamental wave became a little distorted after depletion. In contrast, the beam quality of the Stokes wave was much better. Furthermore, there was no obvious change in the Stokes mode profile with increasing diode power. This phenomenon was similar to the beam clean-up effect [38] that occurs in general Raman lasers in which the Raman radiation almost oscillates as a single transverse mode even when the fundament wave oscillates on several transverse modes. The horizontal and vertical beam quality parameters of the Stokes wave were measured as 1.19 and 1.20, respectively.
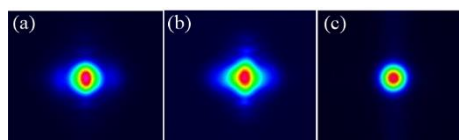
Figure 5. Mode profiles of the (**a**) original fundamental, (**b**) depleted fundamental, and (**c**) Stokes waves.

The pulse waveforms of the fundamental pulse (before and after depletion) and the Stokes pulse were detected by two Si detectors (THORLABS, DET10A/M, 400–1100 nm, Newton, New Jersey, United States). An oscilloscope (Tektronix, TDS5052B, 500MHz, 5GS/s, Bracknell, Berkshire, United Kingdom) was used to record the pulse temporal behaviors. The SPS threshold was 64 W. Figure 6a shows the temporal characteristics of the original fundamental, depleted fundamental, and Stokes pulses under a

diode power of 70 W. The fundamental pulse was depleted at the falling edge. The Stokes pulse rose at the point where the fundamental wave depletion commenced. The build-up time of the Stokes pulse was about 82 ns. The fundamental pulse widths (all pulse widths were full width half maximum) before and after depletion were 131 ns and 91 ns, respectively. The Stokes pulse width was 22 ns. With increasing diode power, the fundamental depletion was stronger. The pulse widths of the depleted fundamental and Stokes waves decreased. The time interval between the fundamental and Stokes pulses also decreased because the Stokes pulse needed less time to accumulate in the Stokes cavity under higher pump power. Figure 6b shows the temporal characteristics of the original fundamental, depleted fundamental, and Stokes pulses under a diode power of 98 W. The fundamental pulse was significantly consumed just after it passed through the peak. This corresponds to the optimum condition in which the majority of the stored accumulated population inversion in the gain medium Nd:YAG was extracted through Q-switching into the circulating fundamental field. The fundamental pulse widths before and after depletion were 110 ns and 46 ns, respectively. The Stokes pulse width was 12 ns. The time interval between the fundamental and Stokes pulses was about 73 ns.
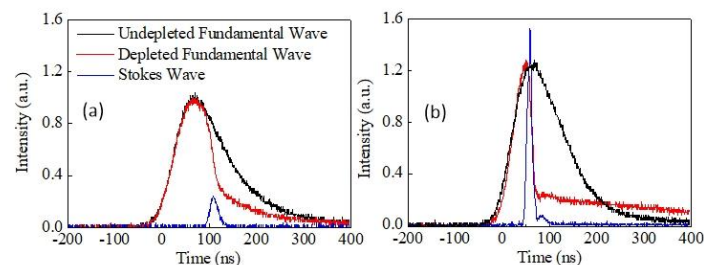
Figure 6. Waveforms of the fundamental (before and after depletion) and Stokes pulses under diode powers of (**a**) 70 W and (**b**) 98 W.

4. Conclusions

A KTP crystal was used as the nonlinear medium in an intracavity SPS source. With a desire to improve the average THz output power, the diode-side pumped configuration was employed to obtain a high intracavity fundamental power and a large fundamental beam size. The fundamental cavity was designed as a convex–plane configuration to offset some of the thermal effect and further increase the interaction volume among the fundamental, Stokes, and THz waves. The THz wave was efficiently emitted from the KTP crystal by adopting a surface-emitted configuration. The generated THz frequency could be tuned from 3.19 THz to 5.94 THz with three gaps. The optimal THz frequency was 5.74 THz where the average THz power was maximal. The fundamental beam diameter in the KTP crystal was about 1.3 mm. Finally, the maximum THz output power of 166 μW at 5.74 THz was obtained under a diode power of 98 W, and the fundamental wave depletion increased to 51%. Compared with the diode-end pumped configuration reported using the KTP crystal, the maximum average THz output power was more than doubled.

Conflicts of Interest: The authors declare no conflicts of interest.

References

1.   Shoji, I.; Kondo, T.; Shirane, A.M.; Ito, R. Absolute scale of second-order nonlinear-optical coefficients. *J. Opt. Soc. Am.* **1997**, *14*, 2268–2294. [CrossRef]

2.   Hildenbrand, A.; Wagner, F.R.; Akhouayri, H.; Natoli, J.Y.; Commandre, M.; Théodore, F.; Albrecht, H. Laser-induced damage investigation at 1064 nm in KTiOPO$_4$ crystals and its analogy with RbTiOPO$_4$. *Appl. Opt.* **2009**, *48*, 4263–4269. [CrossRef] [PubMed]

3.   Driscoll, T.A.; Hoffman, H.J.; Stone, R.E.; Perkins, P.E. Efficient second-harmonic generation in KTP crystals. *J. Opt. Soc. Am. B* **1986**, *3*, 683–686. [CrossRef]

4.   Brown, A.J.; Bowers, M.S.; Kangas, K.W.; Fisher, C.H. High-energy, high-efficiency second-harmonic generation of 1064-nm radiation in KTP. *Opt. Lett.* **1992**, *17*, 109–111. [CrossRef] [PubMed]

5.   Stolzenberger, R.A.; Hsu, C.C.; Peyghambarian, N.; Reid, J.J.; Morgan, R.A. Type II sum frequency generation in flux and hydrothermally grown KTP at 1.319 and 1.338 μm. IEEE Photon. *Technol. Lett.* **1989**, *1*, 446–448. [CrossRef]

6.   Chen, Y.F.; Chen, Y.S.; Tsai, S.W. Diode-pumped Q-switched laser with intracavity sum frequency mixing in periodically poled KTP. *Appl. Phys. B* **2004**, *79*, 207–210. [CrossRef]

7.   Kato, K. Parametric oscillation at 3.2 μm in KTP pumped at 1.064 μm. *IEEE J. Quantum Electron.* **1991**, *27*, 1137–1140. [CrossRef]

8.   Lin, J.T.; Montgomery, J.L. Generation of tunable mid-IR (1.8–2.4 μm) laser from optical parametric oscillation in KTP. *Opt. Commun.* **1990**, *75*, 315–320. [CrossRef]

9.   Su, F.F.; Zhang, X.Y.; Wang, W.T.; Cong, Z.H.; Shi, M.; Yang, X.Q.; Kong, W.J.; Ma, L.L.; Wu, W.D. High-efficient diode-pumped actively Q-switched Nd: YAG/KTP Raman laser at 1096 nm wavelength. *Opt. Commun.* **2013**, *305*, 201–203. [CrossRef]

10. Lee, C.Y.; Chang, C.C.; Sung, C.L.; Chen, Y.F. Intracavity continuous-wave multiple stimulated-Raman-scattering emissions in a KTP crystal pumped by a Nd:YVO$_4$ laser. *Opt. Express* **2015**, *23*, 22765–22770. [CrossRef]

11. Wang, W.T.; Cong, Z.H.; Chen, X.H.; Zhang, X.Y.; Qin, Z.G.; Tang, G.Q.; Li, N.; Wang, C.; Lu, Q.M. Terahertz parametric oscillator based on KTiOPO$_4$ crystal. *Opt. Lett.* **2014**, *39*, 3706–3709. [CrossRef] [PubMed]

12. Yan, C.; Wang, Y.Y.; Xu, D.G.; Xu, W.T.; Liu, P.X.; Yan, D.X.; Duan, P.; Zhong, K.; Shi, W.; Yao, J.Q. Green laser induced terahertz tuning range expanding in KTiOPO$_4$ terahertz parametric oscillator. *Appl. Phys. Lett.* **2016**, *108*, 011107. [CrossRef]

13. Wu, M.H.; Chiu, Y.C.; Wang, T.D.; Zhao, G.; Zukauskas, A.; Laurell, F.; Huang, Y.C. Terahertz parametric generation and amplification from potassium titanyl phosphate in comparison with lithium niobate and lithium tantalite. *Opt. Express* **2016**, *24*, 25964–25973. [CrossRef] [PubMed]

14. Wang, Y.Y.; Ren, Y.C.; Xu, D.G.; Tang, L.H.; He, Y.X.; Song, C.; Chen, L.Y.; Li, C.Z.; Yan, C.; Yao, J.Q. Energy scaling and extended tunability of a ring cavity terahertz parametric oscillator based on KTiOPO$_4$ crystal. *Chin. Phys. B* **2018**, *27*, 114213. [CrossRef]

15. Kawase, K.; Shikata, J.I.; Ito, H. Terahertz wave parametric source. *Phys. D Appl. Phys.* **2002**, *35*, R1. [CrossRef]

16. Shikata, J.I.; Kawase, K.; Karino, K.I.; Taniuchi, T.; Ito, H. Tunable terahertz-wave parametric oscillators using LiNbO$_3$ and MgO:LiNbO$_3$ crystals. *IEEE Trans. Microw. Theory Tech.* **2000**, *48*, 653–661. [CrossRef]

17. Lee, A.; He, Y.; Pask, H. Frequency-Tunable THz Source Based on Stimulated Polariton Scattering in Mg:LiNbO$_3$. *IEEE J. Quantum Electron.* **2013**, *49*, 357–364. [CrossRef]

18. Wang, W.T.; Zhang, X.Y.; Wang, Q.P.; Cong, Z.H.; Chen, X.H.; Liu, Z.J.; Wang, C. Multiple-beam output of a surface-emitted terahertz-wave parametric oscillator by using a slab MgO:LiNbO$_3$ crystal. *Opt. Lett.* **2014**, *39*, 754–757. [CrossRef]

19. Tang, G.Q.; Cong, Z.H.; Qin, Z.G.; Zhang, X.Y.; Wang, W.T.; Wu, D.; Zhang, S.J. Energy scaling of terahertz-wave parametric sources. *Opt. Express* **2015**, *23*, 4144–4152. [CrossRef]

20. Zhang, R.L.; Qu, Y.C.; Zhao, W.J.; Liu, C.; Chen, Z.L. Si-prism-array coupled terahertz-wave parametric oscillator with pump light totally reflected at the terahertz-wave exit surface. *Opt. Lett.* **2016**, *41*, 4016–4019. [CrossRef]

21. Ortega, T.A. Frequency Extension of Solid-State Terahertz Lasers. Ph.D. Thesis, Macquarie University, Sydney, Australia, 2017.

22. Edwards, T.J.; Walsh, D.; Spurr, M.B.; Rae, C.F.; Dunn, M.H.; Browne, P.G. Compact source of continuously and widely-tunable terahertz radiation. *Opt. Express* **2006**, *14*, 1582–1589. [CrossRef] [PubMed]

23. Walsh, D.A.; Browne, P.G.; Dunn, M.H.; Rae, C.F. Intracavity parametric generation of nanosecond terahertz radiation using quasi-phase-matching. *Opt. Express* **2010**, *18*, 13951–13963. [CrossRef] [PubMed]

24. Lee, A.J.; Pask, H.M. Continuous wave, frequency-tunable terahertz laser radiation generated via stimulated polariton scattering. *Opt. Lett.* **2014**, *39*, 442–445. [CrossRef] [PubMed]

25. Ortega, T.A.; Pask, H.M.; Spence, D.J.; Lee, A.J. Stimulated polariton scattering in an intracavity RbTiOPO4 crystal generating frequency-tunable THz output. *Opt. Express* **2016**, *24*, 10254–10264. [CrossRef] [PubMed]

26. Ortega, T.A.; Pask, H.M.; Spence, D.J.; Lee, A.J. THz polariton laser using an intracavity $Mg:LiNbO_3$ crystal with protective teflon coating. *Opt. Express* **2017**, *25*, 3991–3999. [CrossRef] [PubMed]

27. Lee, A.J.; Spence, D.J.; Pask, H.M. Tunable THz polariton laser based on 1342 nm wavelength for enhanced terahertz wave extraction. *Opt. Lett.* **2017**, *42*, 2691–2694. [CrossRef] [PubMed]

28. Tidwell, S.C.; Seamans, J.F.; Bowers, M.S.; Cousins, A.K. Scaling CW diode-end-pumped Nd:YAG lasers to high average powers. *IEEE J. Quantum Electron.* **1992**, *28*, 997–1009. [CrossRef]

29. Welford, D.; Rines, D.M.; Dinerman, B.J. Efficient TEM_{00}-mode operation of a laser-diode side-pumped Nd: YAG laser. *Opt. Lett.* **1991**, *16*, 1850–1852. [CrossRef]

30. Konno, S.; Fujikawa, S.; Yasui, K. 80W cw TEM_{00} 1064 nm beam generation by use of a diode-side-pumped Nd:YAG rod laser. *Appl. Phys. Lett.* **1997**, *70*, 2650–2651. [CrossRef]

31. Yi, J.; Moon, H.J.; Lee, J. Diode-pumped 100-W green Nd:YAG rod laser. *Appl. Opt.* **2004**, *43*, 3732–3737. [CrossRef]

32. Xu, D.; Wang, Y.; Li, H.; Yao, J.; Tsang, Y.H. 104 W high stability green laser generation by using diode laser pumped intracavity frequency-doubling Q-switched composite ceramic Nd:YAG laser. *Opt. Express* **2007**, *15*, 3991–3997. [CrossRef] [PubMed]

33. Li, S.T.; Zhang, X.Y.; Wang, Q.P.; Zhang, X.L.; Cong, Z.H.; Zhang, H.N.; Wang, J.Y. Diode-side-pumped intracavity frequency-doubled Nd: $YAG/BaWO_4$ Raman laser generating average output pow of 3.14 W at 590 nm. *Opt. Lett.* **2007**, *32*, 2951–2953. [CrossRef] [PubMed]

34. Li, C.Y.; Bo, Y.; Yang, F.; Wang, Z.C.; Xu, Y.T.; Wang, Y.B.; Gao, H.W.; Peng, Q.J.; Cui, D.F.; Xu, Z.Y. 106.5 W high beam quality diode-side-pumped Nd:YAG laser at 1123 nm. *Opt. Express* **2010**, *18*, 7923–7928.

35. Kojima, T.; Yasui, K. Efficient diode side-pumping configuration of a Nd:YAG rod laser with a diffusive cavity. *Appl. Opt.* **1997**, *36*, 4981–4984. [CrossRef]

36. Golla, D.; Knoke, S.; Schöne, W.; Ernst, G.; Bode, M.; Tünnermann, A.; Welling, H. 300-W cw diode-laser side-pumped Nd:YAG rod laser. *Opt. Lett.* **1995**, *20*, 1148–1150. [CrossRef] [PubMed]

37. Wang, W.T.; Cong, Z.H.; Liu, Z.J.; Zhang, X.Y.; Qin, Z.G.; Tang, G.Q.; Li, N.; Zhang, Y.G.; Lu, Q.M. THz-wave generation via stimulated polariton scattering in $KTiOAsO_4$ crystal. *Opt. Express* **2014**, *22*, 17092–17098. [CrossRef] [PubMed]

38. Murray, J.T.; Austin, W.L.; Powell, R.C. Intracavity Raman conversion and Raman beam cleanup. *Opt. Mater.* **1999**, *11*, 353–371. [CrossRef]